

WOO-CHUL JUNG¹, JOO-HEON PARK¹, SANG-MIN YOON¹, YOUNG KYUN KIM^{1*}

EFFECT OF MICROSTRUCTURE AND MECHANICAL PROPERTIES OF AL 3003 ALLOY WELD BY STATIONARY SHOULDER FRICTION STIR WELDING PROCESS

The lap joint welding of Al 3003 alloy by stationary shoulder friction stir welding (SSFSW) was performed under the conditions of tool rotation and welding speed, and it was confirmed that the welding was performed under all conditions. The tunnel defects and pores were formed in the weld zone at the lowest tool rotation and welding speed, and it is increased, the weld surface has been improved. At the same tool rotation speed at the welding speed is increased, the grain size was refined in the stir zone (SZ) and thus the hardness increased by about 14% compared to the base metal. The tensile shear strength is measured to be 10 kN or more under most conditions, and in the 4000 rpm with high heat input, the shear tensile strength was measured relatively lower than other conditions due to excessive heat input of the material.

Keywords: Stationary shoulder friction stir welding; Aluminum 3003 alloy; Microstructure; Mechanical properties

1. Introduction

Aluminum alloy is widely used material in industry such as IT convergence, mobile and electronic devices due to its light weight and high corrosion resistance [1]. However, Aluminum products that require welding have high thermal conductivity, it is not easy to control the amount of heat input with general welding, and the low strength at high temperatures and cracks are easy to form during welding, which can cause defects in the welded [2,3]. For this reason, friction stir welding (FSW) process developed by the Welding Institute of UK in 1991 was applied to aluminum alloy welding.

The FSW is a welding technology used in various industries because it can weld materials that cannot be welded by conventional welding methods as a novel solid-state joining process. In particular, stationary shoulder friction stir welding (SSFSW) process can give low and uniform heat input in the welded zone because the shoulder part does not rotate compared to fsw process [4,5]. For this reason, researches on welding of various Al alloys such as Al 7xxx, Al 6xxx, and Al 2xxx have been conducted using SSFSW process, but the researches on SSFSW welding of Al 3xxx series are rare [6,7]. Al 3003 alloy requires high-quality welding such as chemical equipment, fuel tanks, automobile filler tubes, and cooling blocks of batteries due to its moderate strength, excellent machining and corrosion resistance [8].

In this study, the mechanical properties and microstructure of Al 3003 lap joint welding by SSFSW were observed under the conditions of tool rotation speed and welding speed. After SSFSW at welding speeds of 800, 1000, and 2000 mm/min and tool rotation speeds of 2500, 3500, and 4000 rpm, the effects of SSFSW parameters on formability of weld, microstructure, hardness and tensile shear strength properties were investigated. This research will provide the basis for the lap joint SSFSW process of Al 3003 alloys.

2. Experimental

The base material was 3003-H12 Aluminum alloy plate with 3mm thickness. During welding, the Al 3003 alloy plate was lapped by 50 mm and the welding range was set to 200 mm including the initial acceleration section. The used tool employs a conical-threaded probe with a bottom diameter of 3.0 mm, top diameter of 4.2 mm, and 3.7 mm in height and during the welding process, the tool was operated with a tilt angle of 3 degree and load of tool was 6.1 kN. The welding parameters used in this study are summarized in Table 1.

After welding, the specimens were prepared in the order of welding cutting, mounting, grinding, and etching according to the general preparation process. After etching, the microstructure

¹ ADVANCED MATERIAL & PROCESSING CENTER, INSTITUTE FOR ADVANCED ENGINEERING, 175-28 GOAN-RO, 51 BEON-GIL, YONGIN-SI, GYEONGGI, 17180, KOREA

* Corresponding author: kyk@iae.re.kr



was observed with an optical microscope (OM, Nikon, ECLIPSE MA100, Japan), scanning electron microscope (SEM, Tescan, MIRA3 LMH, Czech Republic) and the grain size of the stirring zone was analyzed with electron backscatter diffraction (EBSD, AMETEK, Velocity Super, USA). After SEM analysis, the size of the precipitate in the specimen was analyzed using the Image J software. The tensile shear test according to KS B 0801 by making a specimen, and tested by universal test machine (UTM, MTS Sintech 30/G, USA) at a speed of 2 mm/min. The vickers hardness tests (MATSUZAWA, MMT-3, Japan) were performed at intervals of 0.4 mm from the center of the joint under a load of 100 gf.

TABLE 1

SSFSW parameters of Al 3003 alloy

Sample	Tool rotation speed (rpm)	Welding speed (mm/min)
1	2500	800
2	2500	1000
3	2500	2000
4	3500	800
5	3500	1000
6	3500	2000
7	4000	800
8	4000	1000
9	4000	2000

3. Results and discussion

Fig. 1 shows the cross section of the specimen after SSFSW welding. The faster tool speed and the slower welding speed,

the welded surface had an excellent surface as a result of visual inspection. The fixed shoulder, a characteristic of SSFSW, minimizes the formation of burrs on both surfaces of the welded part, and the fast welding speed is expected to form relatively more burrs compared to the slow welding speed because the shoulder stays in the welded area for a short time. Therefore, SSFSW under suitable weld conditions can obtain a smooth and fine surface that does not require additional surface treatment. Under all conditions, the nugget had a bowl shape due to the conical-threaded probe profile and onion ring shape formed typically in friction welding.

As the amount of heat input increases, the width of the nugget was increased. And tunnel defects and pores were observed in conditions of 2500 rpm-2000 mm/min with the lowest heat input. This means that the frictional heat is not completely transferred to the joint due to the low heat input, so the weld zone is not completely stirred, and tunnel defects and micropores are formed inside.

Fig. 2 shows the microstructure of high heat input (4000 rpm-800 mm/min), medium heat input (3500 rpm-1000 mm/min), and low heat input (2500 rpm-2000 mm/min) conditions. According to the heat input conditions, deformed microstructure was observed at SZ and it was confirmed that the precipitates of $Al_6(Mn, Fe)$ was distributed. In general, in Al-Mn based alloys, $Al_6(Mn, Fe)$ is a reinforcing phase and it is reported that it affects the hardness of the material according to the size or distribution of the precipitates [9]. Fig 3 shows the SEM image and image J analyzed the average size of precipitates. As a result of the analysis of the average size of precipitates in SZ, the size of 4.07 μm under high heat input conditions, 3.36 μm under the medium input condition, and 2.91 μm under low heat input con-

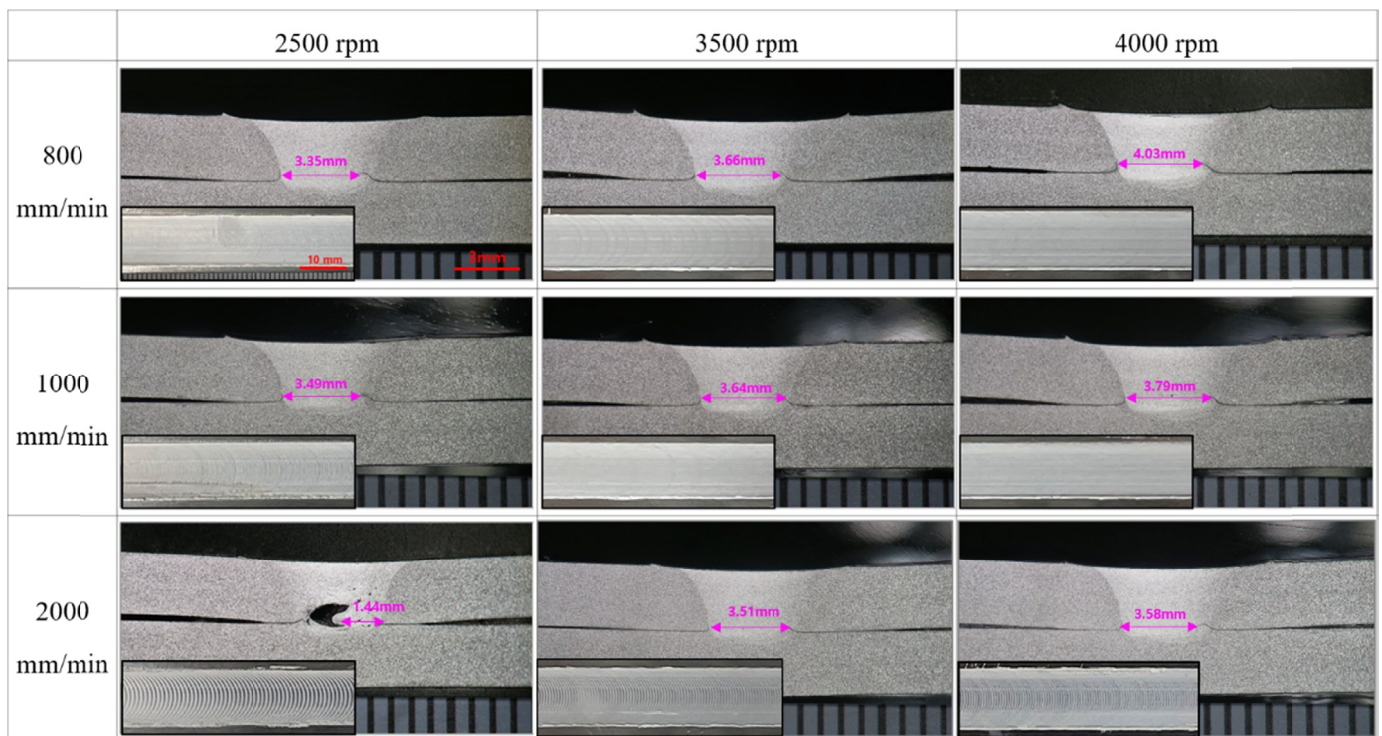


Fig. 1. Surface and Cross-section images of weld zone after SSFSW

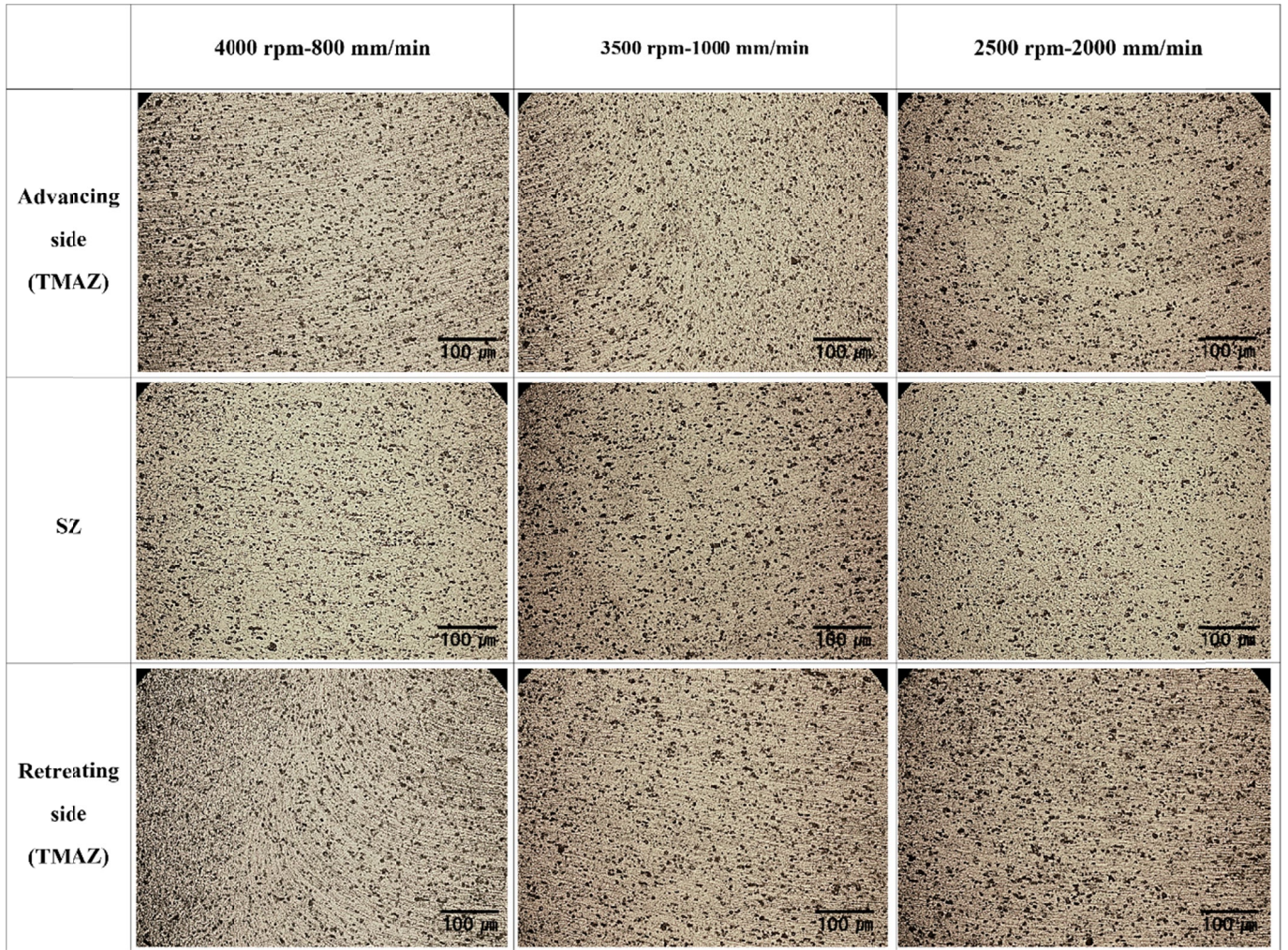


Fig. 2. Microstructure image by heat input condition and welding zone

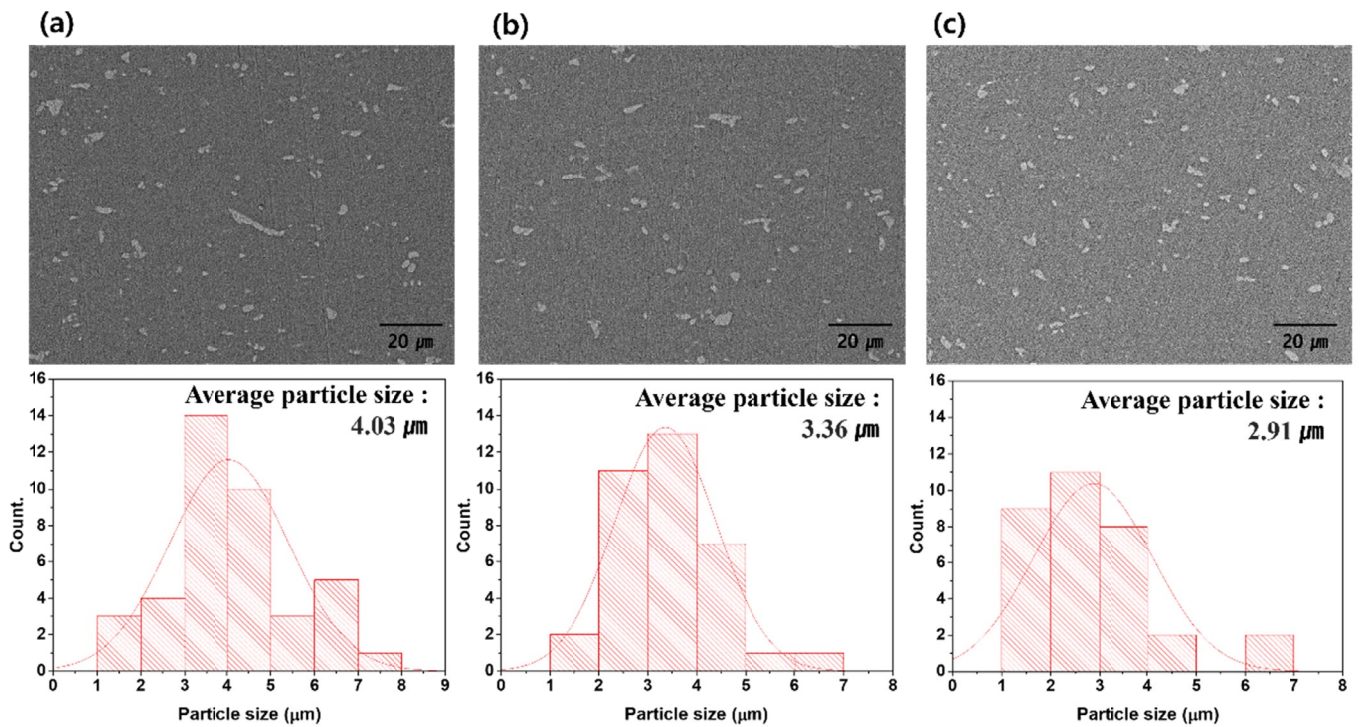


Fig. 3. The average particle size analyzed by SEM image using Image J software; (a) 4000 rpm-800 mm/min, (b) 3500 rpm-1000 mm/min and (c) 2500 rpm-2000 mm/min

ditions were observed. The faster the cooling speed, the smaller the size of the precipitates, And the smaller the precipitates, the more it affects the increase in hardness (as is shown in Fig. 5). The TMAZ was formed on both sides of the SZ of the weld, and in the low heat input condition, the microstructure of TMAZ was relatively less deformed. This indicates that the material becomes soft due to the relatively high energy input under high and medium heat input conditions, and the flow of the material is easily deformed, and the energy input increases as the tool rotation speed increases and the welding speed decreases.

Fig. 4 shows the EBSD inverse pole figure(IPF) and grain boundary(GB) map analysis results for each welding speed condition with a tool rotation speed of 3500 rpm. It was confirmed that fine grains were formed in the SZ due to dynamic recrystallization under all conditions, and the grain size decreased as the welding speed increased. A fast welding speed means that the cooling rate is fast and the crystal nucleation is faster than the grain growth rate, so the grains are refined. The

smallest grains are formed at 2.06 μm under the conditions of 3500 rpm-2000 mm/min. In the GB map analysis, it was confirmed that the faster the moving speed under the same rpm conditions, the low-angle grain boundaries($\theta < 15^\circ$) decreased, while the fraction of high-angle grain boundaries increased. Another literature reported the high-angle grain boundary suppresses the slip deformation of the crystal and can increase the strength of the material at the grain boundary [10]. However, in the EBSD analysis results, it was confirmed that the refinement of grain size changes to a greater width than the grain boundary angle, and it was judged that the effect of grain size is more dominant in the increase of mechanical properties.

Fig. 5 shows the hardness and tensile shear strength of the joint of weld specimen. In Fig. 5(a), as the rotation speed of the tool increases at a welding speed of 1000 mm/min, the hardness of the SZ increases, but the hardness decreases at 4000 rpm. As the tool rotation speed increases, the thermal effect is large, and the hardness was measured to be relatively low due to soften-

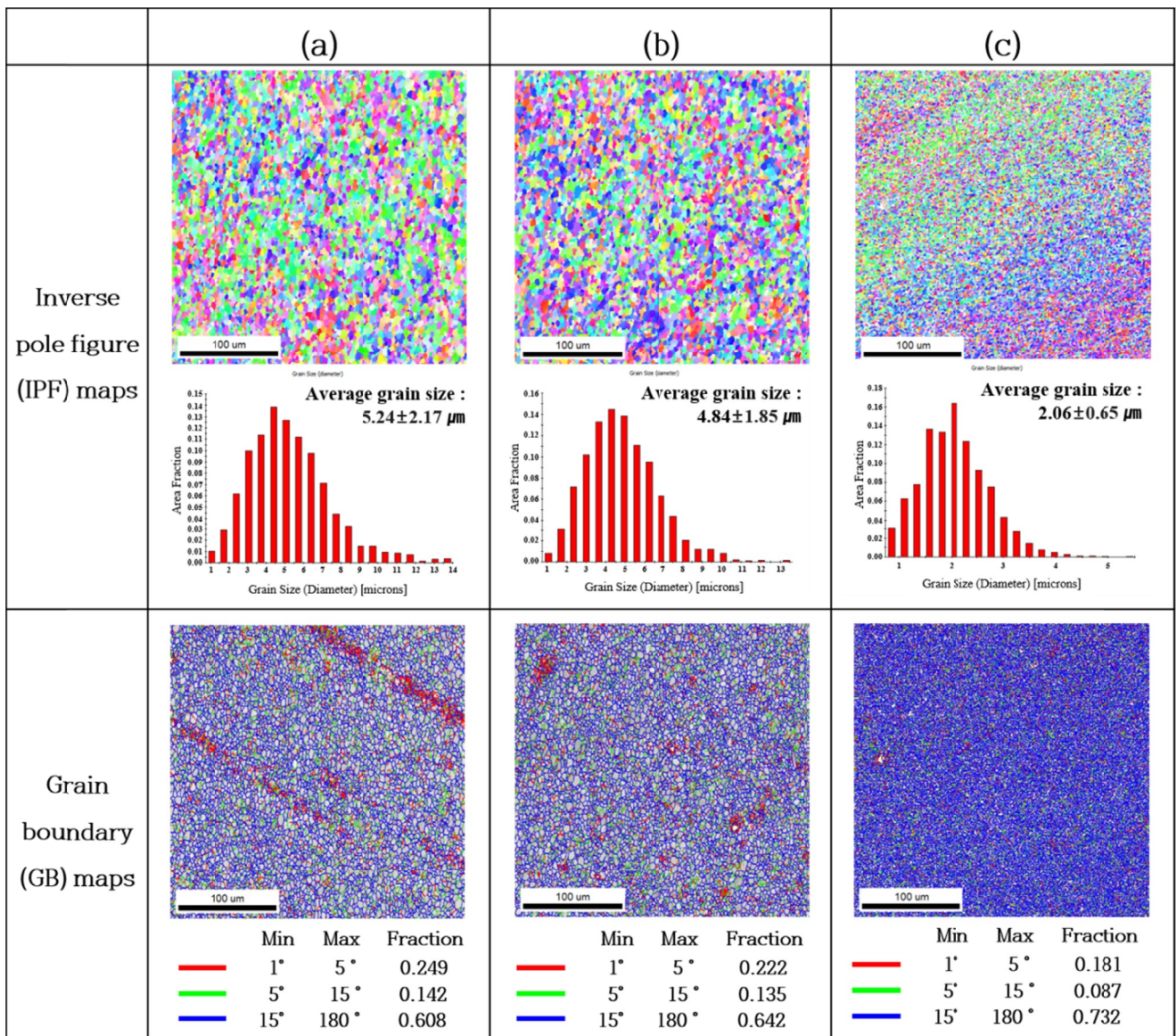


Fig. 4. EBSD IPF patterns and GB map analysis results of stir zone by weld speed condition of 3500 rpm; (a) 800 mm/min, (b) 1000 mm/min and (c) 2000 mm/min

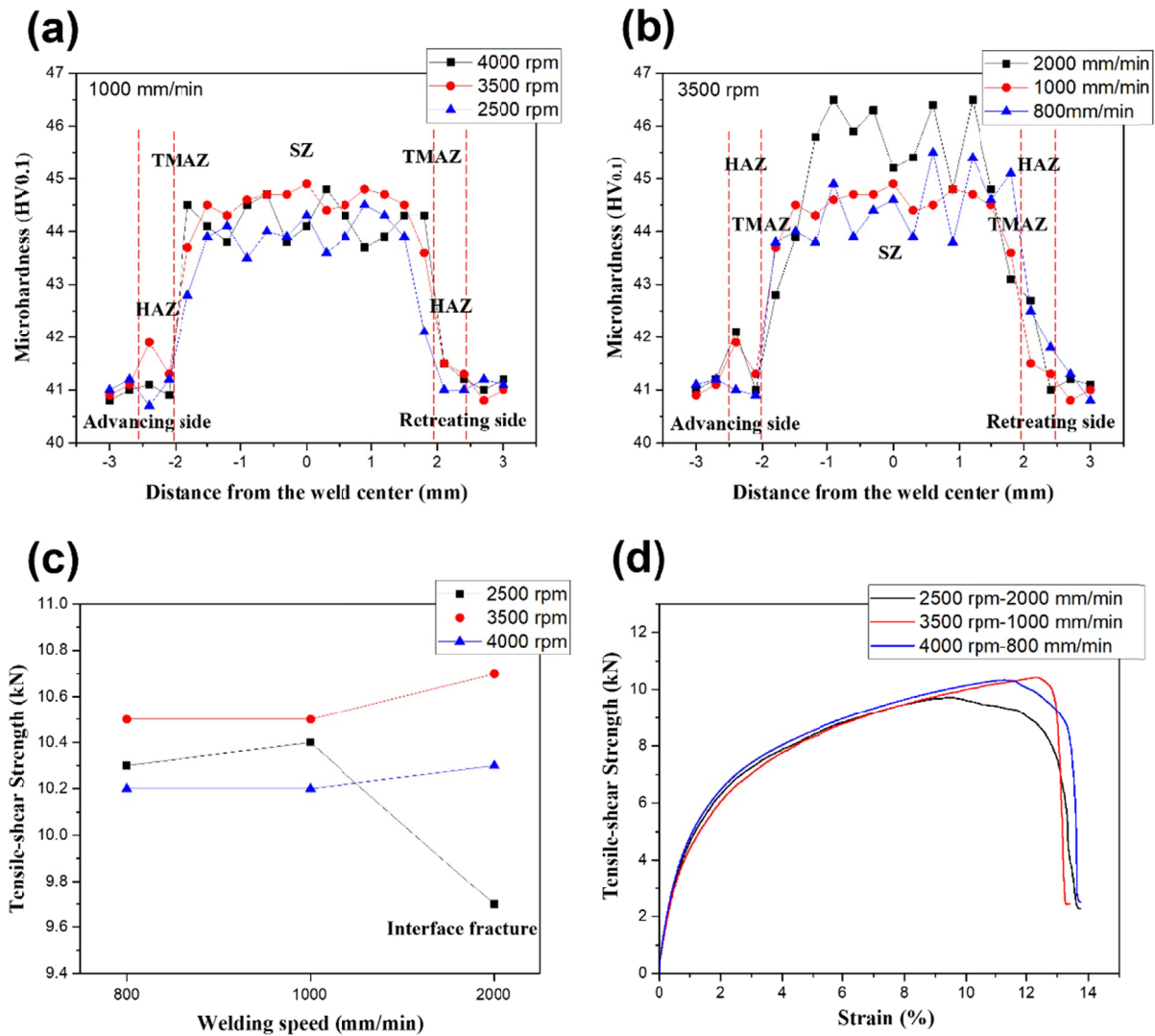


Fig. 5. Hardness profile and tensile shear strength properties according to SSFSW conditions; (a) Hardness profile under the condition of tool rotation speed, (b) Hardness profile under welding speed conditions, (c) Tensile shear strength properties and (d) Stress-strain curve according to heat input conditions

ing of the weld. In TMAZ and HAZ, the hardness was decreased and reached the hardness of the base metal.

In Fig. 5(b), the welding speed of 2000 mm/min, which formed the finest grains at the same tool rotation speed, had the highest hardness. In addition, it is presumed that the small precipitates by fast cooling rate have had some affect on the increase of hardness. The hardness value of SZ was measured overall uniformly in the conditions of 3500 rpm-1000 mm/min. This means that the distribution of the heat by the stirring force and pressure applied to the material is constant.

Fig. 5(c) and (d) shows the tensile shear strength of the specimen. It had tensile shear strength ranges from a minimum of 9.7 kN to a maximum of 10.8 kN. In general, the occurrence of interface fracture in lap joint welding occurs when the width of the interface junction is narrower than the thickness of the base material [11].

The sample welded under the condition of 2500 rpm-2000 mm/min had a tunnel defect in the SZ and showed fracture shape at the interface. It had 9.7 kN of the shear tensile strength.

Other conditions, fracture occurred near TMAZ and the tensile shear strength was measured to be more than 10 kN. The shear tensile strength was increased in faster welding speed at the same tool rotation speed and at the tool rotation speed of 3500 rpm, the shear tensile strength was the highest of 10 kN or more. The shear tensile strength was relatively decreased under the conditions of the fastest tool rotation speed of 4000 rpm, and the material is softened due to excessive heat input above the appropriate energy, resulting in low shear tensile strength.

Fig. 6 shows the SEM analysis of the fracture surface of the specimen after the tensile shear test. high heat input and medium heat input conditions show the form of ductile fracture. Fig. 6(a) and (b) contain second phase particles in dimples, and these second phase particles cause micropores. These pores add up to each other and cause ductile fracture [12]. The medium heat input specimen has a rougher around dimples and more severe deformation than the relatively high heat input specimen, and in the tensile shear test, it was confirmed that the medium heat input specimen was deformed by greater stress than the

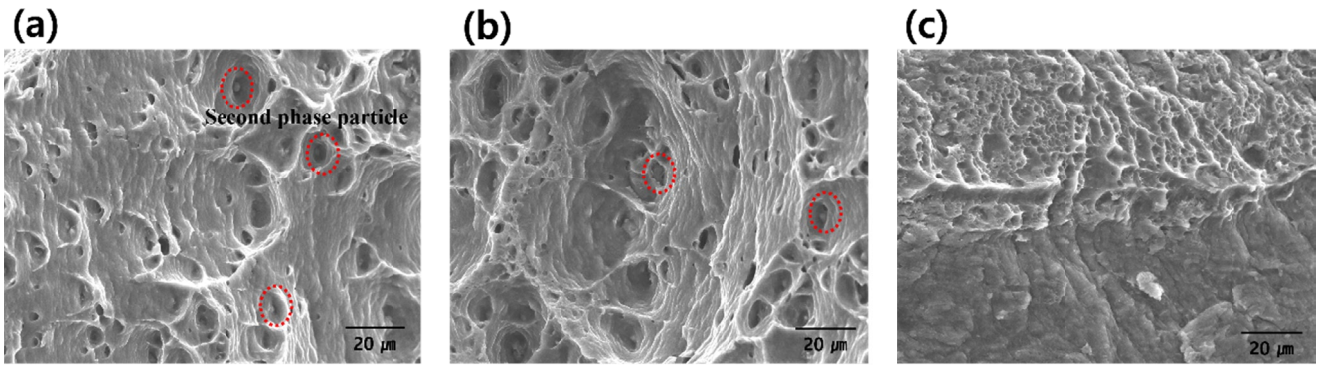


Fig. 6. Fracture surface Analysis of Tensile Shear Specimens According to SSFSW Conditions; (a) 4000 rpm-800 mm/min, (b) 3500 rpm-1000 mm/min and (c) 2500 rpm-2000 mm/min

high heat input specimen. The low heat input specimen in which the interface fracture occurred was not completely stirred, so ductile fracture and brittle fracture were mixed.

4. Conclusions

In this study, the mechanical properties and microstructure of Al3003 lap joint welding by SSFSW were observed under the various conditions of the rotation and welding speed of the tool. The faster welding speed in the state where the heat input to the material was not sufficient formed tunnel defects and micropores in the weld zone. At the same tool rotation speed, the faster the welding speed, the finer grains are formed in the SZ, increasing the hardness and shear tensile strength. Only the faster the welding speed, the finer grains were formed in the SZ. So the hardness and shear tensile strength is increased. In Al 3003 lap joint welding with SSFSW process, the better the surface condition can be obtained as the increase of heat input, but excessive heat input causes defects in the mechanical properties of the material. Therefore, it is necessary to comprehensively satisfy the quality such as surface, strength, and internal defects with the SSFSW process of the appropriate heat input.

Acknowledgments

This work was supported by the Technology Innovation Program (or Industrial Strategic Technology Development Program- Automobile industry technology development) (20015803, High performance composite-based

battery pack case for electric vehicles via hybrid structure and weight lightening technology) funded By the Ministry of Trade, Industry & Energy (MOTIE, Korea).

REFERENCES

- [1] M.D. Tier, T.S. Rosendo, J.A. Mazzaferro, C.P. Mazzaferro, J.F. dos Santos, T.R. Strohaecker, *Int. J. Adv. Manuf. Technol.* **90** (1-4), 267-276 (2017).
- [2] R. Jhon, K.V. Jata, K. Sadananda, *Int. J. Fatigue* **25** (9-11), 939-948 (2003).
- [3] R.S. Mishra, Z.Y. Ma, *Mater. Sci. Eng. R* **50** (1-2), 1-78 (2005).
- [4] W.M. Thomas, E.D. Nicholas, *Mater. Des.* **18** (4-6), 269-279 (1997).
- [5] A. Goloborodko, T. Ito, X. Yun, Y. Motohashi, G. Itoh, *Mater. Trans.* **45** (8), 2503 (2004).
- [6] F. Acerra, G. Buffa, L. Fratini, G. Troiano, *Int. J. Adv. Manuf. Technol.* **48**, 1149-1157 (2010).
- [7] L. Cui, X. Yang, G. Zhou, X. Xu, Z. Shen, *Mater. Sci. Eng. A* **543**, 58-68 (2012).
- [8] Z.P. Xing, S.B. Kang, H.W. Kim, *J. Mater. Sci.* **39**, 1259-1265 (2004).
- [9] M.S. Baek, K.J. Euh, C.Y. Jeong, K.A. Lee, *Korean J. Met. Mater.* **59** (11), 1-6 (2021).
- [10] G. Sun, X. Wei, D. Shang, S. Chen, L. Long, X. Han, *Metals* **10** (12), 1610 (2020).
- [11] A. Roy, C. Mabru, J. L. Gacougnolle, P. Davies, *Appl. Compos. Mater.* **4** (2), 95-119 (1997).
- [12] D. Li, X. Yang, L. Cui, F. He, H. Shen, *Mater. Des.* **64**, 251-260 (2014).